


ORIGINAL ARTICLE

Exosome-delivered circSATB2 targets the miR-330-5p/PEAK1 axis to regulate proliferation, migration and invasion of lung cancer cells

Jun Zhu¹ | Fudong Wang² | Yuan Weng² | Jun Zhao^{1,3} 

¹Department of Thoracic Surgery, The First Affiliated Hospital of Soochow University, Medical College of Soochow University, Suzhou, China

²Department of Thoracic Surgery, Affiliated Hospital of Jiangnan University, Wuxi, Jiangsu, China

³Institute of Thoracic Surgery, The First Affiliated Hospital of Soochow University, Suzhou, China

Correspondence

Jun Zhao, Department of Thoracic Surgery, The First Affiliated Hospital of Soochow University, Medical College of Soochow University, No.899 Pinghai Road, Gusu District, Suzhou City, 215002, Jiangsu Province, China.
Email: zhaojun0327@163.com

Abstract

Exosomes can carry various kinds of RNAs to mediate intercellular communication. Circular RNA (circRNA) special AT-rich sequence-binding protein 2 (circSATB2) was identified as an oncogene in lung cancer. This study was performed to explore the association of circSATB2 with exosomes and the regulatory mechanism of circSATB2. Exosomes could transmit circSATB2 into lung cancer cells. Exosomes enhanced cell proliferation, invasion, and migration by carrying circSATB2. Exosomal circSATB2 abrogated the inhibitory effect of short hairpin (sh)-circSATB2 on lung cancer progression. Moreover, circSATB2 promoted tumor growth in vivo via exosomes. CircSATB2 interacted with microRNA-330-5p (miR-330-5p) and miR-330-5p targeted pseudopodium enriched atypical kinase 1 (PEAK1). In addition, circSATB2 affected the PEAK1 level via sponging miR-330-5p in lung cancer cells. All results suggested that exosomal transfer of circSATB2 contributed to the malignant development of lung cancer by acting as a sponge of miR-330-5p to upregulate PEAK1.

KEYWORDS

circSATB2, exosomes, lung cancer, miR-330-5p, PEAK1

INTRODUCTION

Lung cancer is the most common cause of cancer-induced deaths around the world.¹ Tumor metastasis usually leads to the therapeutic failure in lung cancer patients and the survival rates in different regions are from 4% to 17%.^{2,3} The targeted therapies are important for lung cancer screening and treatment.⁴ The new biological targets remain to be discovered in lung cancer. Exosomes are extracellular nanometric vesicles that can function as key players of intercellular communication in tumor microenvironment.⁵ Exosomes can transmit various types of molecules, such as RNAs, DNAs, proteins, and lipids.⁶ In addition, exosomes have been found to be associated with diagnosis and therapy of lung cancer.⁷

Circular RNAs (circRNAs) are stable closed-loop RNAs derived from back-splicing of pre-messenger RNAs.⁸ The previous research indicated that circRNAs participated in the biological processes of lung cancer, including proliferation, apoptosis, migration and invasion.⁹ CircRNAs are

enriched in exosomes and exo-circRNAs have potentially been used for clinical management of cancers.¹⁰ CircRNA special AT-rich sequence-binding protein 2 (circSATB2, hsa_circ_0008928) has been validated to promote the malignant development in non-small cell lung cancer, and it was abnormally expressed in serum exosomes of lung cancer patients.¹¹ The further relation between circSATB2 and exosome in lung cancer needs to be studied.

CircRNAs serve as natural sponges for microRNAs (miRNAs) to regulate gene levels, consequently affecting cancer biology and progression.¹² Shi et al.¹³ found that circSATB2 increased cisplatin resistance and facilitated malignant phenotypes of lung cancer cells via upregulating hexokinase 2 (HK2) through sponging miR-488. The recent studies demonstrated that microRNA-330-5p (miR-330-5p) induced the anti-cancer regulation in lung cancer.^{14,15} Pseudopodium enriched atypical kinase 1 (PEAK1) was reported to accelerate tumor invasion and metastasis in lung cancer.^{16,17} CircSATB2/miR-330-5p/PEAK1 network has never been researched in lung cancer.

This research aimed to investigate the involvement of exo-circSATB2 in lung cancer and the downstream molecular signals of circSATB2. CircSATB2 was assumed to regulate the expression of PEA1 via binding to miR-330-5p. A series of experiments were performed to explore exo-circSATB2/miR-330-5p/PEAK1 axis in lung cancer cells.

MATERIALS AND METHODS

Human cells

Lung cancer cell lines (H1299, H460, A549), human bronchial epithelial cell line BEAS-2B and embryonic kidney cell line 293T were cultured with Dulbecco's modified eagle medium (DMEM) (Gibco) including 10% newborn bovine serum (Gibco) and 1% penicillin/streptomycin (Gibco) in a 5% CO₂ incubator at 37°C. All cell lines were purchased from BioVector NTCC.

Cell transfection

The circSATB2 and PEA1 sequences were inserted into the pCD5-ciR vector (GENESEED) and pcDNA vector (GENESEED) to obtain the overexpression vector OE-circSATB2 and pcDNA-PEAK1, respectively. The stable lentiviral vector of circSATB2 with short hairpin RNA (shRNA) (sh-circSATB2) and the negative control (sh-NC) were purchased from RIBOBIO. The miR-330-5p mimic, miR-330-5p inhibitor, and the controls (mimic NC, inhibitor NC) were also provided by RIBOBIO. After cell seeding (1×10^4) into the 48-well plates overnight, cells with 70% confluence were transfected with the mixture of vectors or RNAs using Lipofectamine 3000 Kit (Invitrogen).

Exosome extraction, identification, and co-culture

Exosomes were isolated from H1299 cells through the ultracentrifugation as previously indicated.¹⁸ The morphology observation of exosome was performed under the transmission electron microscopy (TEM) (JEM-1-11; JEOL). Tumor susceptibility gene 101 (TSG101) and lysosomal granular glycoprotein 63 (CD63) were used as protein markers for exosome identification via western blot. Moreover, H460 and A549 cells were incubated with the exosome suspension from H1299 cells for 6 h. Cells were then harvested for further use.

Reverse transcription-quantitative polymerase chain reaction assay

Total RNA was extracted via TRIzol Reagent (Invitrogen), following the user's manual. A total 2 µg RNA was used for each sample. The reverse transcription and level detection of circRNA and mRNA were performed by QuantiTect Reverse

TABLE 1 Primer sequences used for RT-qPCR

Name	Primer sequences (5'-3')
circ_SATB2	Forward: CAAGAGTGGCATTCAACCGC Reverse: CTTTCCGCACCAGGACAAAC
miR-330-5p	Forward: GCCGAGTCTCTGGGCTGTG Reverse: CTCAACTGGTGTCTGGAG
miR-1278	Forward: TCGGCAGGTAGTACTGTGCATA Reverse: CTCGTATCCAGTGCAGGGTC
miR-147b	Forward: GCCGAGGTGTGCCGAAATG Reverse: GCAGGGTCCGAGGTAT
miR-326	Forward: TCGGCAGGCCTCTGGGCCCTTC Reverse: CAGTGCAGGGTCCGAGGTAT
miR-665	Forward: GCCGAGACCAGGAGGCTGAG Reverse: TGGTGTCTGGAGTCGGCAA
PEAK1	Forward: AGTCAGTGTCTAGTTGCTCGG Reverse: GGCTCCAACCTCTGGGCATTA
GAPDH	Forward: GACAGTCAGCCGCATCTTCT Reverse: GCGCCAATACGACCAAATC
U6	Forward: CTCGCTTCGGCAGCACA Reverse: AACGCTTCACGAATTTGCGT

Transcription Kit and QuantiTect SYBR Green PCR Kit (Qiagen). The miRNA expression was quantified using miScript II RT Kit and miScript SYBR Green PCR Kit (Qiagen). CircRNA/mRNA and miRNAs levels were normalized by glyceraldehyde-phosphate dehydrogenase (GAPDH) and U6, followed by the relative expression analysis through the $2^{-\Delta\Delta Ct}$ method.¹⁹ The used primers were shown in Table 1.

Cell counting Kit-8 assay

1×10^4 H460 and A549 cells were incubated with exosomes or transfected with vectors/RNAs. 10 µL Cell Counting Kit-8 (CCK-8) solution (Beyotime) was added to each well for 2 h, and the optical density value was determined at $\lambda = 450$ nm using the microplate reader (Bio-Rad).

EDU assay

The proliferation ability was detected by EDU Imaging Kit (KeyGen) in the treated H460 and A549 cells. In accordance with the manufacturer's instruction, cells were labeled with EDU and cell nuclei were stained with diamidine phenylindole (DAPI). The stained cells were observed under the fluorescence microscope (Olympus). The merged cells by EDU and DAPI staining were regarded as the positive proliferation cells.

Colony formation assay

The 12-well plates were seeded with 5×10^2 /well H460 and A549 cells, and then the plates were incubated at 37°C. After

14 days, the macroscopic colonies were stained with 0.1% crystal violet (Beyotime) and the colony number was measured through the Image J software (National Institutes of Health [NIH]).

Transwell assay

Transwell chamber (Corning) was enveloped with matrigel (Corning), then the upper chamber was inoculated with 1×10^5 cells in serum-free medium. Subsequently, the lower chamber was pipetted into 500 μ L DMEM medium containing 10% fetal bovine serum (FBS). The invaded cells into the lower chamber were stained with 0.1% crystal violet (Beyotime). Cell images were observed at $100 \times$ magnification and cells were counted through an inverted microscope (Olympus).

Wound healing assay

Two straight scratches were produced using a sterile pipette tip in H460 and A549 cells of 6-well plates, then cells were washed by phosphate buffer solution (PBS) (Gibco) and the remaining cells were cultured in 10% FBS + DMEM medium for 24 h. The wound width was examined at 0 h and 24 h. Cell migration ratio was calculated, with the control group as 100%.

Western blot assay

Total protein was extracted by radioimmunoprecipitation assay (RIPA) lysis buffer (Beyotime), then 50 μ g proteins were used for expression determination.²⁰ The primary antibodies against TSG101 (Abcam, ab125011), CD63 (Abcam, ab134045), matrix metalloproteinase 9 (MMP9; Abcam, ab76003), MMP2 (Abcam, ab97779), PEAK1 (Sigma, 09-274), and GAPDH (Abcam, ab181602) were diluted at 1:1000 in Tris buffered saline Tween (TBST). After incubation with goat anti-rabbit IgG H&L secondary antibody (ab205718, 1:5000) for 1 h, BeyoECL Star Kit (Beyotime) was used to visualize the protein bands and ImageJ software (NIH) was applied for expression analysis.

Tumor xenograft assay

A total of 20 BALB/c male nude mice (Vital River Laboratory Animal Technology) were divided into four groups with five mice/group. A549 cells were treated with sh-NC, sh-circSATB2, sh-circSATB2 + vector exo or sh-circSATB2 + OE-circSATB2 exo. The rank of each mouse was subcutaneously injected with 1×10^6 cells and mice were observed for 4 weeks. The width and length of tumors were measured by a digital caliper, and tumor volume ($\text{width}^2 \times \text{length} \times 0.5$) was calculated every week. The flow rate of CO₂ was used to replace the 30% air each minute and then tumors were dissected from the sacrificed mice.

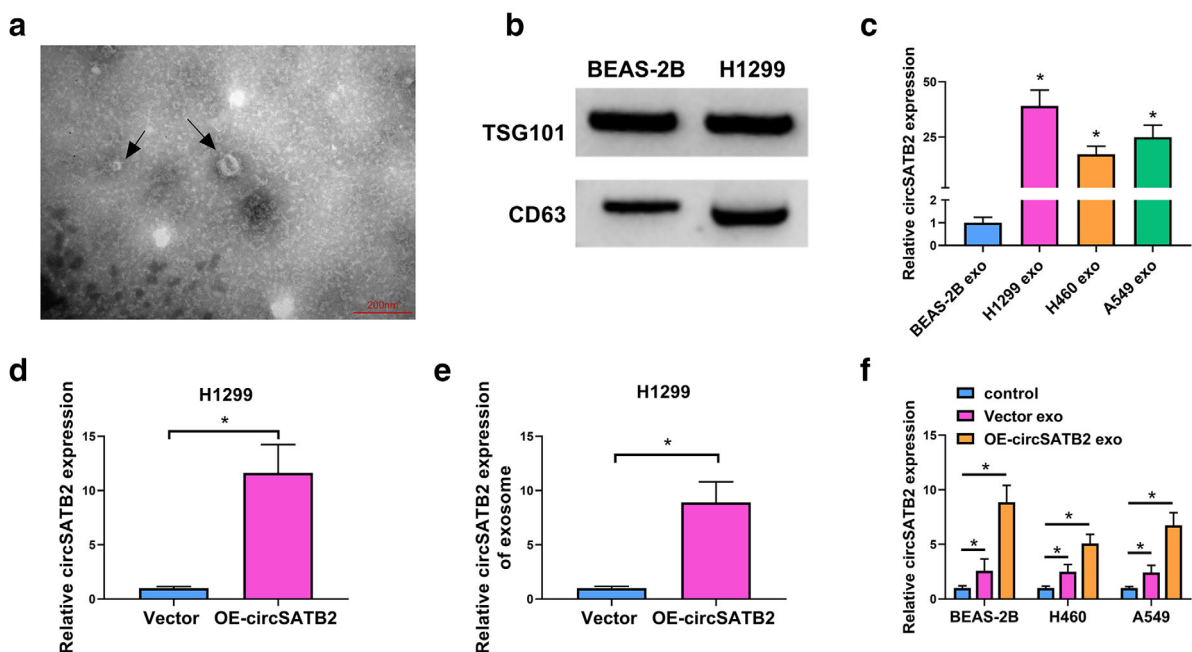


FIGURE 1 Exosomes transferred circSATB2 into lung cancer cells. (a) Exosomes were observed under the TEM. (b) TSG101 and CD63 protein levels in exosomes from BEAS-2B and H1299 cells were detected by western blot. (c) the circSATB2 expression was determined by RT-qPCR in exosomes from BEAS-2B and lung cancer cells. (d) CircSATB2 level was examined by RT-qPCR in H1299 cells with transfection of vector or OE-circSATB2. (e) RT-qPCR was used for circSATB2 quantification in exosomes from vector or OE-circSATB2 transfected H1299 cells. (f) RT-qPCR was performed for expression analysis of circSATB2 in BEAS-2B, H460 and A549 cells after co-culture with vector exosomes or OE-circSATB2 exosomes. * $p < 0.05$. TEM, transmission electron microscopy; RT-qPCR, reverse transcription-quantitative polymerase chain reaction

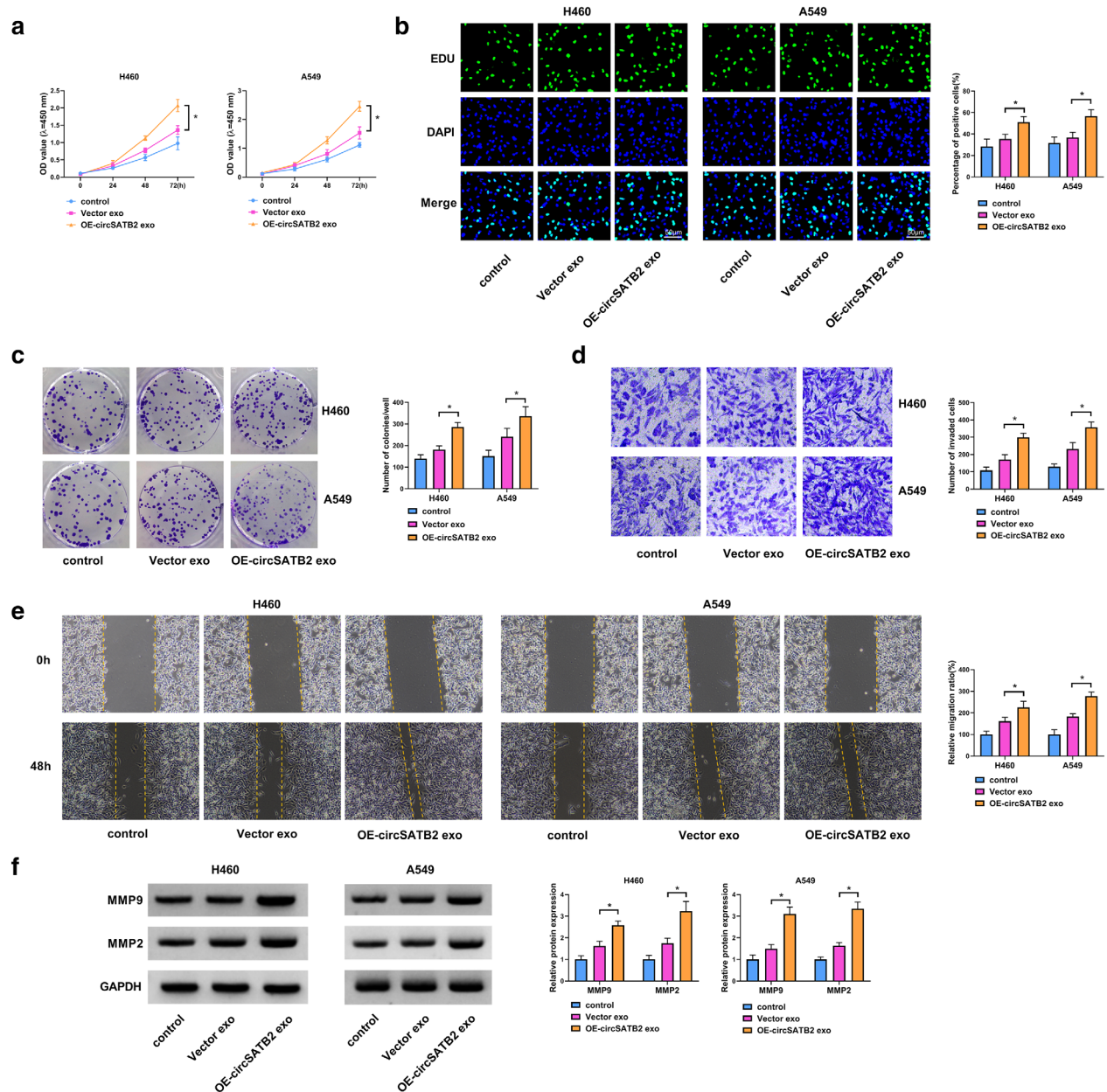


FIGURE 2 Exosomes promoted proliferation, invasion and migration in lung cancer cells via releasing circSATB2. H460 and A549 cells were co-cultured with exosomes from vector or OE-circSATB2 transfected H1299 cells. (a)–(c) the proliferation ability was assessed through CCK-8 assay (a), EDU assay (b) and colony formation assay (c). (d), (e) the invasion (d) and migration (e) capacities were evaluated through transwell assay and wound healing assay. (f) MMP9 and MMP2 protein levels were measured through western blot. $*p < 0.05$. CCK-8, Cell Counting Kit-8; MMP9, matrix metalloproteinase 9; MMP2, matrix metalloproteinase 2

Tumors were weighed on an electronic scale, and circSATB2 expression was quantified by reverse transcription-quantitative polymerase chain reaction (RT-qPCR) in tumor tissues. This animal assay was ratified by the Animal Ethical Committee of Affiliated Hospital of Jiangnan University.

Dual-luciferase reporter assay

The target prediction was carried out using starBase (<http://starbase.sysu.edu.cn>). The circSATB2 sequence (containing

the miR-330-5p binding sites) was cloned into the pmirGLO plasmid (Promega) to construct the wild-type (wt) plasmid circSATB2 wt. The mutant sequence of circSATB2 (containing the mutated sites of miR-330-5p) was inserted into the luciferase plasmid, which was considered as the mutant-type (mut) plasmid circSATB2 mut. The wt and mut sequences of PEAK1 3'UTR were used to construct the PEAK1 3'UTR wt and PEAK1 3'UTR mut plasmids. A total of 293T cells were planted into the 48-well plates, followed by co-transfection of circSATB2 or PEAK1 3'UTR luciferase plasmid and miR-330-5p mimic or mimic NC. The luciferase activity detection

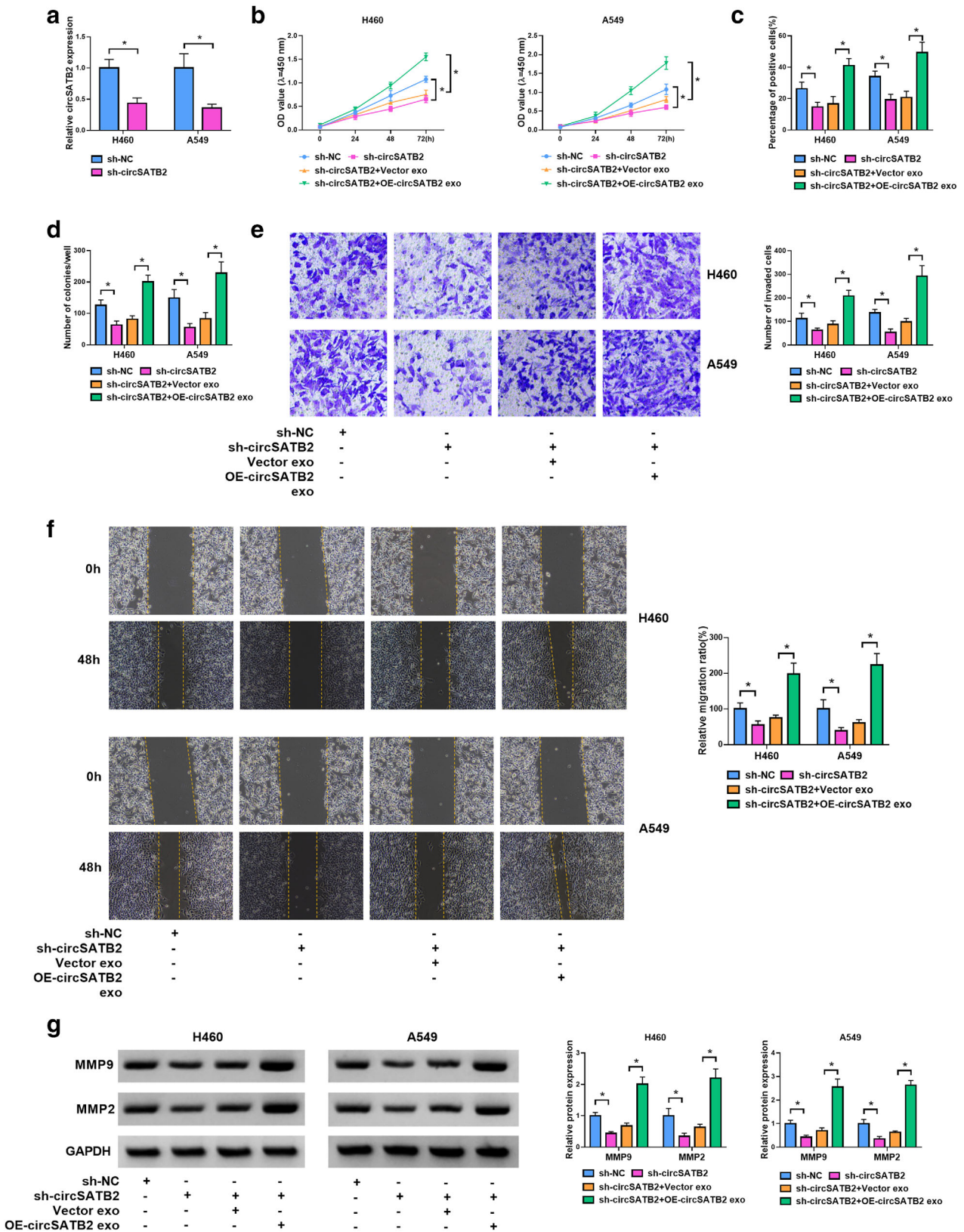


FIGURE 3 Exosomes secreted circSATB2 to abolish the sh-circSATB2-induced cancer inhibition in lung cancer cells. (a) RT-qPCR was applied to examine the circSATB2 expression in sh-NC or sh-circSATB2 transfected H460 and A549 cells. (b)–(g) H460 and A549 cells were treated with sh-NC, sh-circSATB2, sh-circSATB2 + vector exo or sh-circSATB2 + OE-circSATB2 exo. (b)–(d) CCK-8 assay (b), EDU assay (c) and colony formation assay (d) were applied to determine cell proliferation. (e),(f) Transwell assay (e) and wound healing assay (f) were applied to detect cell invasion (e) and migration (f). (g) Western blot was applied to analyze the protein expression of MMP9 and MMP2. **p* < 0.05. RT-qPCR, reverse transcription-quantitative polymerase chain reaction; CCK-8, Cell Counting Kit-8; MMP9, matrix metalloproteinase 9; MMP2, matrix metalloproteinase 2

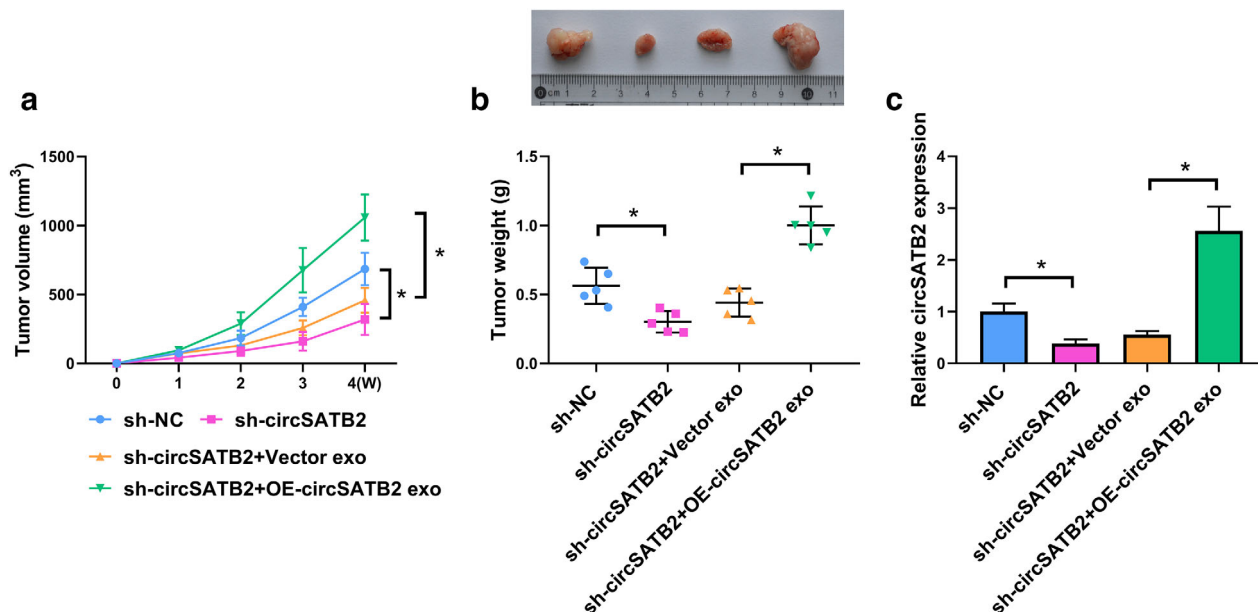


FIGURE 4 Exosomal circSATB2 facilitated tumor growth of lung cancer in vivo. (a),(b) tumor volume (a) and weight (b) were measured in xenograft tumors of sh-NC, sh-circSATB2, sh-circSATB2 + vector exo and sh-circSATB2 + OE-circSATB2 exo groups. (c) CircSATB2 expression of each group was detected by RT-qPCR. * $p < 0.05$.

was performed by the Dual-luciferase Reporter Detection Kit (Promega) after transfection for 48 h.

RNA immunoprecipitation assay

The target binding between circSATB2 and miR-330-5p was analyzed using Imprint RNA Immunoprecipitation Kit (Sigma). The antibody-coated magnetic beads of anti-Argonaute-2 (anti-Ago2) or anti-immunoglobulin G (anti-IgG) group were incubated to 293T cells at 4°C overnight, then circSATB2 and miR-330-5p levels were examined through RT-qPCR. Input group without antibody incubation was used as the positive group.

Statistical analysis

Experiments were performed with three replicates, and data were shown as the mean \pm standard deviation. SPSS 22.0 (SPSS) was applied for statistical analysis, and difference comparison was conducted via Student's *t*-test or analysis of variance (ANOVA) followed by Tukey's test. Importantly, $p < 0.05$ demonstrated that the difference was significant.

RESULTS

Exosomes transferred circSATB2 into lung cancer cells

Exosomes were isolated from lung cancer cells and normal controls. The exosomal morphology was observed under the

TEM, and exosomes were exhibited as the bilayer membrane structures with diameter <100 nm (Figure 1(a)). The exosome markers TSG101 and CD63 were detected in exosomes from BEAS-2B and H1299 cells (Figure 1(b)). We have found that circSATB2 level was upregulated in exosomes derived from H1299, H460, and A549 cells compared with BEAS-2B cells (Figure 1(c)). The expression change of circSATB2 in H1299 exo was the most significant, and then H1299 cells were used for exosome preparation. H1299 cells were transfected with OE-circSATB2 or vector, and RT-qPCR analysis showed that OE-circSATB2 induced the significant circSATB2 overexpression (Figure 1(d)). The exosomes were extracted from transfected H1299 cells, and circSATB2 expression was higher in exosomes of OE-circSATB2 group than that in vector group (Figure 1(e)). The exosomes from H1299 cells were co-cultured with BEAS-2B, H460, and A549 cells. Interestingly, circSATB2 level was significantly increased in BEAS-2B, H460, and A549 cells after co-incubation with OE-circSATB2 exo relative to vector exo and control groups (Figure 1(f)). Therefore, exosomes could transmit circSATB2 into lung cancers.

Exosomes promoted proliferation, invasion, and migration in lung cancer cells via releasing circSATB2

Subsequently, we investigated the function of circSATB2 in lung cancer cells via exosomes. CCK-8 assay showed that cell proliferation was enhanced in H460 and A549 cells after co-culture with exosomes of OE-circSATB2 group, compared to vector exo and control groups (Figure 2(a)). The results of EDU assay (Figure 2(b)) and colony formation assay (Figure 2(c)) revealed

that OE-circSATB2 exosomes promoted the proliferation capacity of H460 and A549 cells. Through the detection of transwell assay and wound healing assay, we observed that exosomes from OE-circSATB2-transfected H1299 cells promoted the invasion (Figure 2(d)) and migration (Figure 2(e)) abilities of H460 and A549 cells. Moreover, western blot analysis demonstrated that MMP9 and MMP2 protein levels were upregulated in OE-circSATB2 exo group contrasted with control and vector exo groups (Figure 2(f)). Taken together, exosomes with circSATB2 could accelerate the progression of lung cancer cells.

Exosomes secreted circSATB2 to abolish the sh-circSATB2-induced cancer inhibition in lung cancer cells

As shown in Figure 3(a), circSATB2 was downregulated in sh-circSATB2 group compared to sh-NC group of H460

and A549 cells. The transected cells were co-cultured with vector exosomes or OE-circSATB2 exosomes. Knockdown of circSATB2 suppressed cell proliferation (Figure 3(b)–(d)), invasion (Figure 3(e)) and migration (Figure 3(f)), whereas these effects were alleviated after the incubation with OE-circSATB2 exosomes. In addition, OE-circSATB2 exosomes eliminated the inhibitory regulation of sh-circSATB2 for MMP9 and MMP2 protein expression in H460 and A549 cells (Figure 3(g)). Therefore, lung cancer progression inhibition caused by circSATB2 downregulation was abrogated via exosomal transfer of circSATB2.

Exosomal circSATB2 facilitated tumor growth of lung cancer in vivo

Xenograft tumor models of sh-NC, sh-circSATB2, sh-circSATB2 + vector exo and sh-circSATB2 + OE-circSATB2

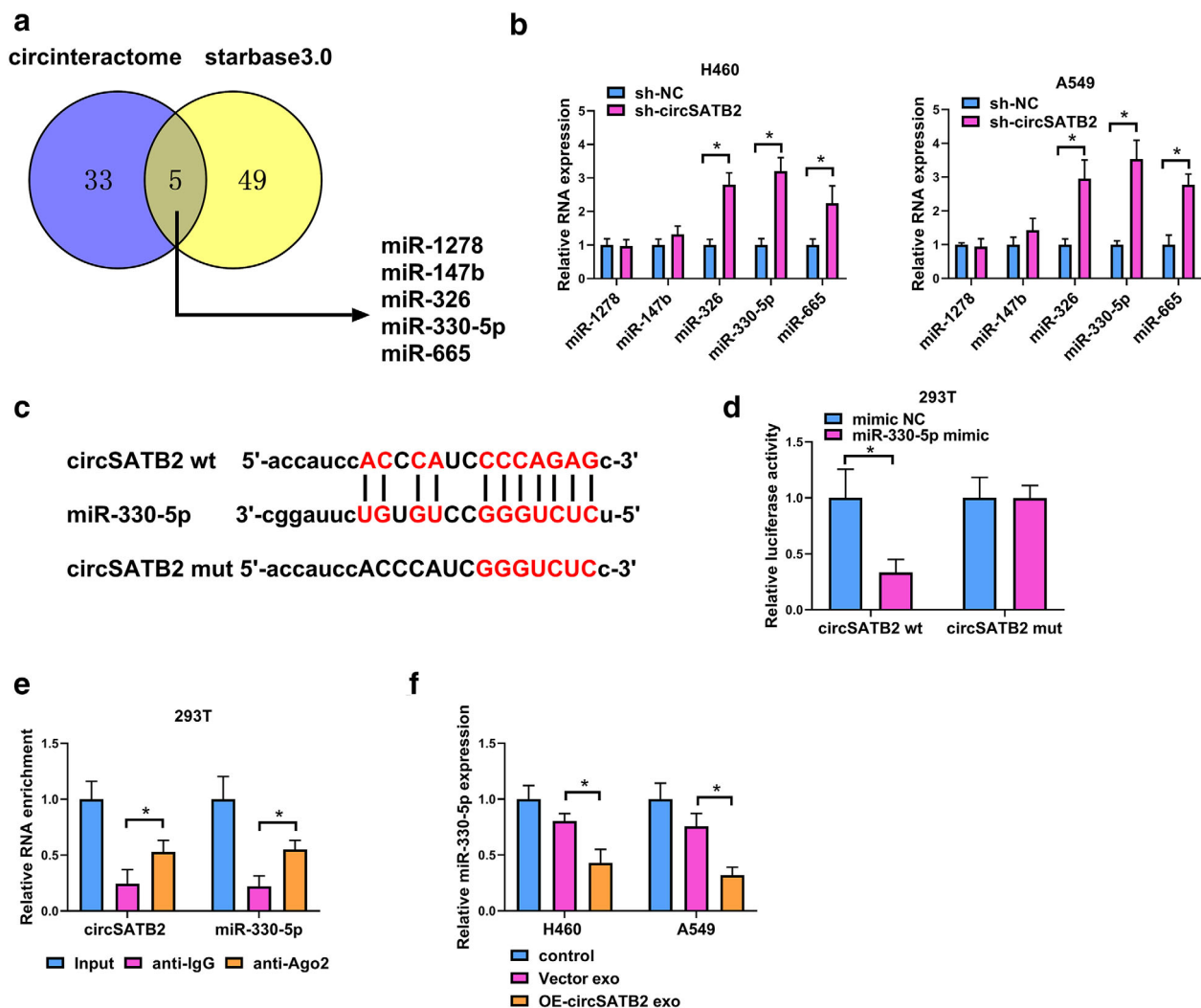


FIGURE 5 CircSATB2 combined with miR-330-5p in lung cancer cells. (a) Venn diagram was used to analyze the mutual miRNA targets of circSATB2 by circinteractome and starBase 3.0. (b) the levels of miR-1278, miR147b, miR-326, miR-330-5p, miR-665 were quantified using RT-qPCR in H460 and A549 cells transfected with sh-NC or sh-circSATB2. (c) the binding sites between circSATB2 and miR-330-5p in starBase 3.0. (d),(e) dual-luciferase reporter assay (d) and RIP assay (e) were conducted to analyze whether circSATB2 interacted with miR-330-5p in 293T cells. (f) the miR-330-5p level was examined by RT-qPCR after co-incubation with vector exosomes or OE-circSATB2 exosomes. * $p < 0.05$. RT-qPCR, reverse transcription-quantitative polymerase chain reaction

exo groups were established in nude mice. Tumor growth curve manifested that tumor volume was reduced by silence of circSATB2, whereas OE-circSATB2 exo relived this inhibition (Figure 4(a)). The excised tumors were exhibited in Figure 4 (b), and tumor weight was also increased in sh-circSATB2 + OE-circSATB2 exo group contrasted to sh-circSATB2 + vector exo group. The incubation with OE-circSATB2 exosomes upregulated the level of circSATB2, relative to alone transfection of sh-circSATB2 (Figure 4(c)). These data suggested that exosomal circSATB2 could promote tumorigenesis of lung cancer in xenograft tumor model.

CircSATB2 combined with miR-330-5p in lung cancer cells

MiRNA targets of circSATB2 were predicted by the online software. As displayed in Figure 5(a), five miRNAs (miR-1278, miR147b, miR-326, miR-330-5p, and miR-665) were simultaneously predicted by circinteractome and starBase 3.0. RT-qPCR screening indicated that miR-330-5p was the most significantly upregulated miRNA after the knockdown of circSATB2 in H460 and A549 cells (Figure 5(b)). The binding sites between circSATB2 and miR-330-5p sequences

were shown as Figure 5(c). The results from dual-luciferase reporter assay manifested that miR-330-5p mimic repressed the luciferase activity of circSATB2 wt plasmid relative to mimic NC group, but that of circSATB2 mut plasmid was not affected in 293T cells (Figure 5(d)). CircSATB2 and miR-330-5p were largely enriched by Ago2 protein compared with IgG control group (Figure 5(e)). In addition, the incubation of OE-circSATB2 exosomes inhibited the level of miR-330-5p in H460 and A549 cells (Figure 5(f)). Overall, miR-330-5p was identified as a target of circSATB2 in lung cancer cells.

CircSATB2 acts as a miR-330-5p sponge to regulate the PEAK1 level

The analysis of starBase 3.0 exhibited the binding region between the sequences of PEAK1 3'UTR and miR-330-5p (Figure 6(a)). Transfection of miR-330-5p mimic and PEAK1 3'UTR wt reduced the luciferase signal of 293T cells, whereas transfection of miR-330-5p mimic and PEAK1 3'UTR mut did not affect the luciferase activity (Figure 6 (b)). PEAK1 protein expression was increased in H460 and A549 cells with the co-culture of exosomes from OE-

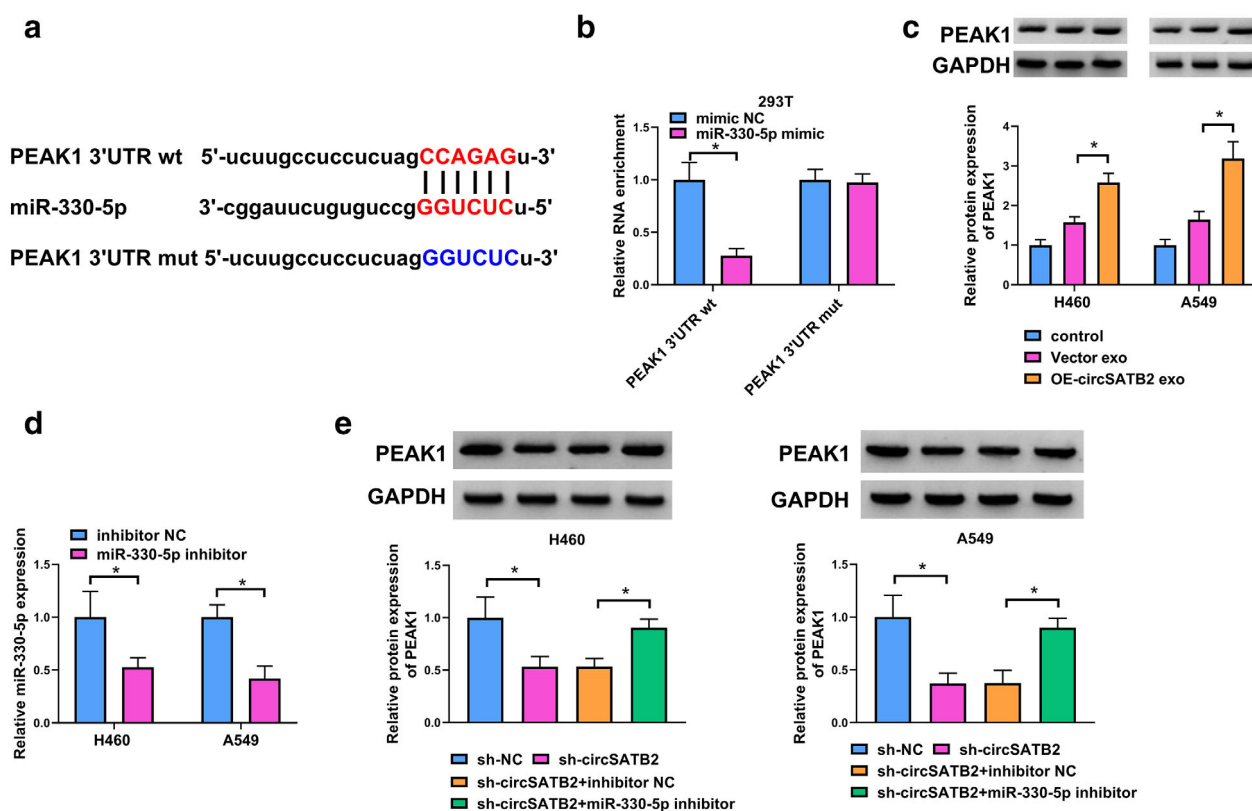


FIGURE 6 CircSATB2 acts as a miR-330-5p sponge to regulate the PEAK1 level. (a) starBase 3.0 showed the binding region between miR-330-5p and PEAK1 3'UTR sequences. (b) The binding analysis between PEAK1 3'UTR and miR-330-5p was determined using dual-luciferase reporter assay in 293T cells. (c) PEAK1 protein expression was measured using western blot after H460 and A549 cells were incubated with exosomes. (d) the transfection efficiency of miR-330-5p inhibitor was assessed by RT-qPCR. (e) the protein detection of PEAK1 was performed via western blot after transfection of sh-NC, sh-circSATB2, sh-circSATB2 + inhibitor NC or sh-circSATB2 + miR-330-5p inhibitor. * $p < 0.05$. PEAK1, pseudopodium enriched atypical kinase 1; RT-qPCR, reverse transcription-quantitative polymerase chain reaction

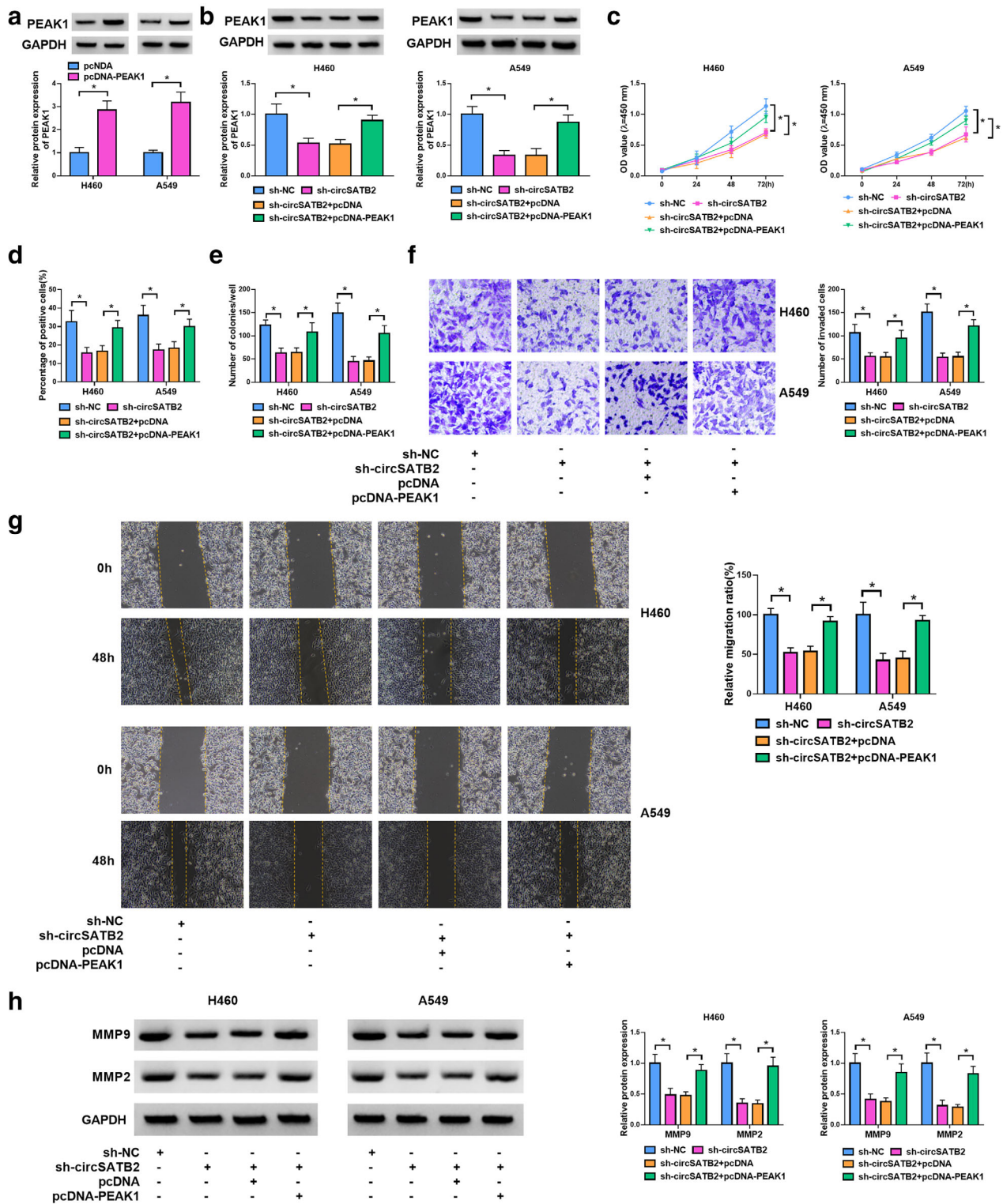


FIGURE 7 PEAK1 overexpression relieves the sh-circSATB2-mediated progression inhibition in lung cancer cells. (a) the protein expression of PEAK1 was analyzed via western blot in pcDNA and pcDNA-PEAK1 groups. (b)–(h) transfection of sh-NC, sh-circSATB2, sh-circSATB2 + pcDNA or sh-circSATB2 + pcDNA-PEAK1 was performed in H460 and A549 cells. (b) PEAK1 protein analysis was conducted via western blot. (c)–(e) the assessment of cell proliferation was carried out via CCK-8 assay (c), EDU assay (d) and colony formation assay (e). (f), (g) cell invasion and migration were evaluated via transwell assay (f) and wound healing assay (g). (h) MMP9 and MMP2 protein examination was performed using western blot. **p* < 0.05. PEAK1, pseudopodium enriched atypical kinase 1; sh-NC, short-hairpin negative control; CCK-8, Cell Counting Kit-8; MMP9, matrix metalloproteinase 9; MMP2, matrix metalloproteinase 2

circSATB2 group (Figure 6(c)). Relative to inhibitor NC transfection, miR-330-5p level was effectively inhibited by miR-330-5p inhibitor in H460 and A549 cells (Figure 6(d)). Additionally, silence of circSATB2 induced the protein downregulation of PEAK1, but this effect was reversed by miR-330-5p inhibitor (Figure 6(e)). Hence, circSATB2 upregulated the expression of PEAK1 via targeting miR-330-5p.

PEAK1 overexpression relived the sh-circSATB2-mediated progression inhibition in lung cancer cells

PEAK1 protein level was much higher in pcDNA-PEAK1 group than that in pcDNA group, showing that transfection efficiency of pcDNA-PEAK1 was significant in H460 and A549 cells (Figure 7(a)). Additionally, pcDNA-PEAK1 has abated the expression downregulation of PEAK1 caused by sh-circSATB2 (Figure 7(b)). The data of CCK-8 assay (Figure 7(c)), EDU assay (Figure 7(d)), and colony formation assay (Figure 7(e)) demonstrated that overexpression of PEAK1 counteracted the sh-circSATB2-induced proliferation inhibition. The inhibitory effects of circSATB2 knockdown on cell invasion (Figure 7(f)), migration (Figure 7(g)), and MMP protein levels (Figure 7(h)) were also mitigated after PEAK1 was upregulated in H460 and A549 cells. These experiments revealed that circSATB2 affected lung cancer progression via upregulating PEAK1.

DISCUSSION

This study elucidated that exosomal circSATB2 acted as an oncogenic regulator in lung cancer via sponging miR-330-5p to upregulate the PEAK1 level, providing the pivotal evidence for the association of circSATB2 with exosomes and miR-330-5p/PEAK1 axis.

Exosomes are nanosized membrane-enveloped vesicles secreted by all kinds of cells, and they can be used as the storage of functional molecules.²¹ Here, we have isolated exosomes from lung cancer cells and TEM observation showed the bilayer membranes of vesicles. The detection of endosomal protein TSG101 and tetraspanin protein CD63 further identified that exosomes were released from cells. CircSATB2 expression upregulation was determined in lung cancer cells after co-culture with exosomes. Exosomes could transfer circSATB2 from the donor cells to the recipient cells.

Increasing studies suggested that circRNAs regulated cancer progression through the exosomal pathway. Wang et al.²² stated that circ_PVT1 induced epithelial-mesenchymal transition in cervical cancer cells via the delivery of exosomes. Chen et al.²³ unraveled that circ_0051443 repressed the biological behaviors of hepatocellular carcinoma cells via exosomes. Exosome-mediated transmit of circ_0044516 served as a biomarker to enhance proliferation and metastasis in prostate cancer cells.²⁴ To explore whether

circSATB2 functioned in lung cancer via the exosome transmission, lung cancer cells were co-cultured with the extracted exosomes from OE-circSATB2 cells. Cell proliferation, invasion, and migration abilities were promoted after incubation with exosomes containing high level of circSATB2. Furthermore, exosomes from OE-circSATB2 cells abolished anticancer response of circSATB2 knockdown in lung cancer cells. Moreover, OE-circSATB2 exosomes alleviated tumor growth inhibition caused by silence of circSATB2 in mice. Taken together, circSATB2 contributed to the malignant progression of lung cancer by depending on the exosomal release.

CircRNAs are known to serve as the molecular sponges of small miRNAs, therefore, inhibiting the interaction between miRNAs and mRNAs to induce the gene expression changes.²⁵ A variety of circRNA/miRNA/mRNA axes have been discovered in human cancers.^{26,27} Additionally, circWHSC1 and circTADA2A suppressed the progression of lung cancer via the miR-296-3p/AKT3 axis and miR-638/KIAA0101 axis.^{28,29} MiR-330-5p was used as a miRNA target for circSATB2 after screening and analysis. Meanwhile, PEAK1 was affirmed as a downstream target for miR-330-5p and circSATB2 resulted in the level upregulation of PEAK1 via targeting miR-330-5p. Additionally, all effects of circSATB2 downregulation were reversed by overexpression of PEAK1 in lung cancers. Therefore, circSATB2 function was related to miR-330-5p-mediated PEAK1 expression. More importantly, exosomal circSATB2 could inhibit miR-330-5p level and promote PEAK1 expression in lung cancer cells. Exosomal circRNA-0001445 aggravated glioma progression through the miR-127-5p/SNX5 and exosome-secreted ciRS-122 promoted chemoresistance in colorectal cancer cells via the miR-122/PKM2 axis.^{30,31} The current data demonstrated that exosome-transmitted circSATB2 contributed to the lung cancer development by the regulation of miR-330-5p/PEAK1 network.

CONCLUSION

In summary, exosomal circSATB2 facilitated cell progression via mediating the miR-330-5p/PEAK1 regulatory axis in lung cancer. Exo-circSATB2 might be an effective biomarker for lung cancer patients.

CONFLICTS OF INTEREST

The authors declare that they have no conflicts of interest.

ORCID

Jun Zhao  <https://orcid.org/0000-0003-2923-7792>

REFERENCES

1. Toumazis I, Bastani M, Han SS, Plevritis SK. Risk-based lung cancer screening: a systematic review. *Lung Cancer*. 2020;147:154–86.
2. Xie S, Wu Z, Qi Y, Wu B, Zhu X. The metastasizing mechanisms of lung cancer: recent advances and therapeutic challenges. *Biomed Pharmacother*. 2021;138:111450.

3. Hirsch FR, Scagliotti GV, Mulshine JL, Kwon R, Curran WJ Jr, Wu YL, et al. Lung cancer: current therapies and new targeted treatments. *Lancet*. 2017;389:299–311.
4. Tan WL, Jain A, Takano A, Newell EW, Iyer NG, Lim WT, et al. Novel therapeutic targets on the horizon for lung cancer. *Lancet Oncol*. 2016;17:e347–e62.
5. Kugeratski FG, Kalluri R. Exosomes as mediators of immune regulation and immunotherapy in cancer. *FEBS J*. 2021;288:10–35.
6. Kok VC, Yu CC. Cancer-derived exosomes: their role in cancer biology and biomarker development. *Int J Nanomedicine*. 2020;15:8019–36.
7. Xu K, Zhang C, Du T, et al. Progress of exosomes in the diagnosis and treatment of lung cancer. *Biomed Pharmacother*. 2021;134:111111.
8. Tang X, Ren H, Guo M, Qian J, Yang Y, Gu C. Review on circular RNAs and new insights into their roles in cancer. *Comput Struct Biotechnol J*. 2021;19:910–28.
9. Chen HH, Zhang TN, Wu QJ, Huang XM, Zhao YH. Circular RNAs in lung cancer: recent advances and future perspectives. *Front Oncol*. 2021;11:664290.
10. Hou J, Jiang W, Zhu L, Zhong S, Zhang H, Li J, et al. Circular RNAs and exosomes in cancer: a mysterious connection. *Clin Transl Oncol*. 2018;20:1109–16.
11. Zhang N, Nan A, Chen L, Li X, Jia Y, Qiu M, et al. Circular RNA circSATB2 promotes progression of non-small cell lung cancer cells. *Mol Cancer*. 2020;19:101.
12. Fu Y, Sun H. Biogenesis, cellular effects, and biomarker value of circHIPK3. *Cancer Cell Int*. 2021;21:256.
13. Shi Q, Ji T, Ma Z, Tan Q, Liang J. Serum exosomes-based biomarker circ_0008928 regulates cisplatin sensitivity, tumor progression, and glycolysis metabolism by miR-488/HK2 Axis in cisplatin-resistant nonsmall cell lung carcinoma. *Cancer Biother Radiopharm*. 2021. <https://doi.org/10.1089/cbr.2020.4490>
14. Ge P, Cao L, Zheng M, Yao Y, Wang W, Chen X. LncRNA SNHG1 contributes to the cisplatin resistance and progression of NSCLC via miR-330-5p/DCLK1 axis. *Exp Mol Pathol*. 2021;120:104633.
15. Wang Y, Xu R, Zhang D, Lu T, Yu W, Wo Y, et al. Circ-ZKSCAN1 regulates FAM83A expression and inactivates MAPK signaling by targeting miR-330-5p to promote non-small cell lung cancer progression. *Transl Lung Cancer Res*. 2019;8:862–75.
16. Ding C, Tang W, Fan X, Wang X, Wu H, Xu H, et al. Overexpression of PEAK1 contributes to epithelial-mesenchymal transition and tumor metastasis in lung cancer through modulating ERK1/2 and JAK2 signaling. *Cell Death Dis*. 2018;9:802.
17. Geng Q, Li Z, Li X, Wu Y, Chen N. LncRNA NORAD, sponging miR-363-3p, promotes invasion and EMT by upregulating PEAK1 and activating the ERK signaling pathway in NSCLC cells. *J Bioenerg Biomembr*. 2021;53:321–32.
18. Zhang Q, Liu RX, Chan KW, Hu J, Zhang J, Wei L, et al. Exosomal transfer of p-STAT3 promotes acquired 5-FU resistance in colorectal cancer cells. *J Exp Clin Cancer Res*. 2019;38:320.
19. Livak KJ, Schmittgen TD. Analysis of relative gene expression data using real-time quantitative PCR and the 2^(-Delta Delta C [T]) method. *Methods*. 2001;25:402–8.
20. Yang C, Mou Z, Zhang Z, Wu S, Zhou Q, Chen Y, et al. Circular RNA RBPMS inhibits bladder cancer progression via miR-330-3p/RAI2 regulation. *Mol Ther Nucleic Acids*. 2021;23:872–86.
21. Alharbi MG, Lee SH, Abdelazim AM, Saadeldin IM, Abomughaid MM. Role of extracellular vesicles in compromising cellular resilience to environmental stressors. *Biomed Res Int*. 2021;2021:9912281.
22. Wang H, Wei M, Kang Y, Xing J, Zhao Y. Circular RNA circ_PVT1 induces epithelial-mesenchymal transition to promote metastasis of cervical cancer. *Aging*. 2020;12:20139–51.
23. Chen W, Quan Y, Fan S, Wang H, Liang J, Huang L, et al. Exosome-transmitted circular RNA hsa_circ_0051443 suppresses hepatocellular carcinoma progression. *Cancer Lett*. 2020;475:119–28.
24. Li T, Sun X, Chen L. Exosome circ_0044516 promotes prostate cancer cell proliferation and metastasis as a potential biomarker. *J Cell Biochem*. 2020;121:2118–26.
25. Panda AC. Circular RNAs act as miRNA sponges. *Adv Exp Med Biol*. 2018;1087:67–79.
26. Xu D, Wu Y, Wang X, Hu X, Qin W, Li Y, et al. Identification of functional circRNA/miRNA/mRNA regulatory network for exploring prospective therapy strategy of colorectal cancer. *J Cell Biochem*. 2020;121:4785–97.
27. Bai S, Wu Y, Yan Y, Shao S, Zhang J, Liu J, et al. Construct a circRNA/miRNA/mRNA regulatory network to explore potential pathogenesis and therapy options of clear cell renal cell carcinoma. *Sci Rep*. 2020;10:13659.
28. Shi F, Yang Q, Shen D, et al. CircRNA WHSC1 promotes non-small cell lung cancer progression via sponging microRNA-296-3p and up-regulating expression of AKT serine/threonine kinase 3. *J Clin Lab Anal*. 2021;35:e23865.
29. Zhang Y, Yao H, Li Y, Yang L, Zhang L, Chen J, et al. Circular RNA TADA2A promotes proliferation and migration via modulating of miR638/KIAA0101 signal in nonsmall cell lung cancer. *Oncol Rep*. 2021;46:201.
30. Han Y, Liu Y, Zhang B, Yin G. Exosomal circRNA 0001445 promotes glioma progression through miRNA-127-5p/SNX5 pathway. *Aging (Albany NY)*. 2021;13:13287–99.
31. Wang X, Zhang H, Yang H, Bai M, Ning T, Deng T, et al. Exosome-delivered circRNA promotes glycolysis to induce chemoresistance through the miR-122-PKM2 axis in colorectal cancer. *Mol Oncol*. 2020;14:539–55.

How to cite this article: Zhu J, Wang F, Weng Y, Zhao J. Exosome-delivered circSATB2 targets the miR-330-5p/PEAK1 axis to regulate proliferation, migration and invasion of lung cancer cells. *Thorac Cancer*. 2022;13(21):3007–17. <https://doi.org/10.1111/1759-7714.14652>